International Journal of Environmental Impacts
https://www.acadlore.com/journals/IJEI

Water Quality Estimation from Total Suspended Solid and Dissolved Oxygen Concentration in Krueng Pase Watershed, North Aceh, Indonesia

Atika Izzaty[1,2], Ichwana Ramli[3,4*], Bambang Bakri[5]

[1] Department of Geodetic Engineering, Hasanuddin University, 92171 Sulawesi Selatan, Indonesia
[2] International Master Program on Natural Hazards Mitigation and Management, National Cheng Kung University, 70101 Tainan City, Taiwan
[3] Master Program of Environmental Management, Syiah Kuala University, 23111 Banda Aceh, Indonesia
[4] Agricultural Engineering Department, Syiah Kuala University, 23111 Banda Aceh, Indonesia
[5] Department of Civil Engineering, Hasanuddin University, 92171 Sulawesi Selatan, Indonesia

* Correspondence: Ichwana Ramli (ichwana.ramli@usk.ac.id)

Received: 05-12-2025 **Revised:** 08-28-2025 **Accepted:** 10-13-2025

Citation: A. Izzaty, I. Ramli, and B. Bakri, "Water quality estimation from total suspended solid and dissolved oxygen concentration in Krueng Pase Watershed, North Aceh, Indonesia," *Int. J. Environ. Impacts.*, vol. 9, no. 1, pp. 62–73, 2026. https://doi.org/10.56578/ijei090106.

Abstract: The functional value of a watershed is often degraded by anthropogenic activities. Land cover changes, urban expansion, and industrial development can significantly affect river water quality. Consequently, rapid and comprehensive monitoring is required to represent conditions across the entire river system. Advances in Earth observation satellite technology provide efficient tools for monitoring natural resources and environmental quality. This study aims to estimate concentrations of Total Suspended Solids (TSS) and Dissolved Oxygen (DO) in the Krueng Pase River Basin, North Aceh, Indonesia, using satellite imagery. The analysis employed Sentinel-2A data acquired during both dry and rainy seasons from 2020 to 2022, with a spatial resolution of 60 m. Concurrent field measurements collected by the Aceh Environmental Service were used for accuracy assessment. The results reveal seasonal variations in sediment levels within the Krueng Pase Watershed. Validation against in situ observations produced Nash–Sutcliffe Efficiency (NSE) values of 0.949 (very good) for Period I and 0.645 (satisfactory) for Period II. Percent Bias (PBIAS) values were 15.668 (very good) and 21.0307 (very good), respectively. These findings are supported by the estimated DO concentrations, which consistently >5 mg/L. Such levels indicate good oxygen conditions, sufficient to sustain productive aquatic biota and showing no evidence of severe pollution. This study demonstrates that satellite imagery-based estimation of TSS and DO concentrations is a reliable approach for land and water management, particularly in evaluating water pollution.

Keywords: Water quality; Total Suspended Solid; Dissolved Oxygen; Sentinel-2A; Krueng Pase Watershed

1 Introduction

To determine Sediment load volume and evaluate the health of aquatic ecosystems, suspended solid models are commonly applied to measure water quality parameters [1]. Human activities alter the water cycle through land use changes, as well as the construction of dams and reservoirs, which contribute to increased erosion [2]. Erosion processes elevate turbidity, thereby accelerating sedimentation within dams and reducing the overall capacity of watersheds. Rapid population growth further exacerbates environmental problems and intensifies water pollution [3–5]. Total Suspended Solids (TSS) represent a key biogeochemical parameter used to manage water resources and assess water quality [6]. The concentration of TSS is influenced by both natural processes and anthropogenic factors. Within watersheds, suspended solids serve as indicators of contamination levels and sediment transport dynamics. Sedimentation refers to the deposition of debris in water as a direct consequence of erosion. Several environmental analyses have been conducted using laboratory based gravimetric techniques [7]. Deposition occurs when soil particles transported by water currents settle after reaching their settling velocity. This process typically occurs in agricultural fields, riverbeds, reservoir bottoms, and estuarine areas. In watersheds characterized by diverse land use and land cover types, land degradation can substantially influence sedimentation rates [8].

In addition, several water quality parameters can be detected within the watersheds. Sediments often contain substances whose concentrations can be measured, including those associated with biological and chemical factors in surface water or indicative of pollution [9]. Because the collection of these different types of data is typically conducted independently, matched datasets combining remote sensing and in situ water quality measurements remain limited. Multiple parameters can serve as indices of water quality and can be detected terrestrially using algorithms. Examples include Dissolved Oxygen (DO), which is influenced by water temperature, and chlorophyll-a (Chl-a), which indicates the presence of microorganisms in aquatic environments originating from agricultural runoff or sewage [10].

The dynamics and geomorphology of shallow waters are influenced by the total suspended mass. In tidal environments, biophysical processes regulate the transport of sediments and other suspended materials. When integrated with computational algorithms, remote sensing data can be applied to monitor water quality. This technology serves as an effective tool for detecting the distribution of TSS and for accurately monitoring water quality. Although remote sensing does not directly measure changes in sedimentation, it remains one of the most effective methods for detecting and predicting water quality in aquatic systems, including watersheds [11, 12]. By utilizing optical data, TSS concentrations can be estimated with high spatial and temporal resolutions [7].

In the Krueng Pase watershed, increasingly variable surface runoff patterns underscore the need for a mapping system to monitor water quality distribution. This requirement is particularly critical in disaster-prone areas, such as the Krueng Pase watershed, which experiences recurrent flooding during the rainy season. Flood events transport runoff from mountains and cause accumulation in nearby coastal cities. To address this issue, the water index [13] was first calculated using the Normalized Difference Water Index (NDWI) approach to distinguish between open water bodies, reservoirs, and permanent water. The NDWI masking results were then used as input for determining suspended solids and DO levels. Consequently, TSS and DO calculations were restricted to locations identified through the water index.

Two primary remote sensing approaches are generally employed to estimate TSS: direct calculation using remote sensing reflectance (Rrs) and methods based on the reflectance of water-leaving radiance [14, 15]. The technique utilizing Rrs values at specific wavelengths is widely applicable across diverse water types. In this study, four wavelengths (551, 671, 745, and 862 nm) were used to determine TSS concentrations from the Rrs data [16].

Remote sensing for DO detection is also applied to map water quality and pollution. Satellite imagery enables the recording of regional conditions using onboard sensors, thereby facilitating the detection of surface characteristics and their content. Because suspended solids are particles present in water, DO measurements provide complementary information by indicating oxygen availability and overall ecosystem health. However, many national water quality monitoring programs were not originally designed to incorporate satellite overpasses or remote sensing acquisitions [17].

DO is a critical parameter for describing water quality; however, maintaining a monitoring system requires substantial labor and cost. Consequently, technologies with high spatial and temporal resolutions are needed to support effective management plans [18]. Remote sensing has become an important tool for water quality monitoring due to its advantages of broad coverage, regularity, and dynamic observation capabilities. It can be used to monitor changes in water quality in near real time [19].

The purpose of this study was to develop an algorithm based on Sentinel-2A imagery to estimate TSS concentrations and DO distribution within the watershed. By integrating remote sensing methods, the analysis of both TSS and DO parameters became more robust, enabling more accurate water quality assessments. Reflectance values derived from the imagery were compiled into a mathematical model [20] that mapped the distribution of TSS and DO at the pixel level. This pixel by pixel calculation provides an optimal indication of TSS and DO levels in water.

2 Study Materials

2.1 Study Area

The Krueng Pase Basin in Aceh Province is divided into six districts: Aceh Tengah, Pidie, Bener Meriah, Bireun, Aceh Utara, and Nagan Raya. It is located between coordinates $4°30'38''$–$97°02'40''$ and $5°16'34''$–$96°27'12''$. The watershed is predominantly situated in North Aceh and Bireun (Figure 1). The Krueng Pase River serves as an important source of irrigation for the surrounding communities. The basin covers an area of 2,557.8 km^2, draining multiple districts due to its extensive geographical reach.

The river flows through mountainous terrain and passes through several sub-districts and villages. Various developments have emerged around the watershed, including community-built infrastructure within the basin. Technical irrigation projects along the Krueng Pase have been constructed to support agricultural activities, enabling the irrigation of approximately 8,922 hectares of rice fields. This is particularly significant because the river edges are dominated by rice fields, which serve as vital agricultural areas for the local population.

Regarding the socio-economic conditions of the community around the Krueng Pase Watershed, the downstream area is a densely populated urban zone located near the coastline. A significant influx of people from rural areas has migrated to the city center, which functions as an industrial and commercial hub. In contrast, vegetated and

agricultural lands dominate the central part of the watershed. The middle to upstream areas are sparsely populated, and the majority of residents rely on farming as their primary livelihood. These agricultural lands are primarily converted into rice fields and vegetated plots, and their produce is exported or distributed to the city's trading centers.

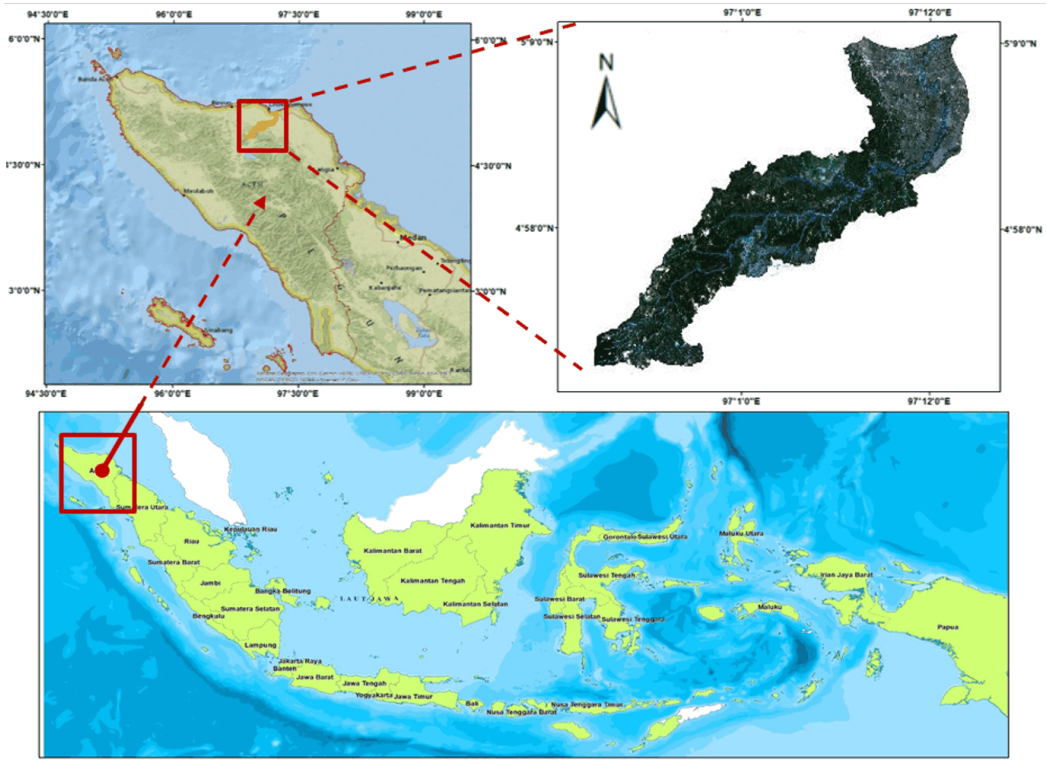

Figure 1. Research location

Due to the extensive forest cover with high vegetation density, Krueng Pase Watershed falls under the Type D climate classification according to Schmidt–Ferguson, which designates temperate regions with seasonal forest vegetation. From a physical and environmental perspective, Krueng Pase Watershed is characterized by high rainfall and dense forest conditions. These forests, although ecologically significant, also contribute to forest degradation in Aceh. Such degradation influences the hydrological response of the watershed, where river flows are surrounded by high-vegetation forests that regulate water dynamics in the region.

2.2 Data Collection

This study utilized Sentinel-2A Level-1C imagery acquired between 2020 and 2022, together with vector datasets delineating the administrative boundaries of the Krueng Pase Watershed. The vector data were obtained from the Indonesian Earth Map at a scale of 1:25,000. Satellite images were accessed through the Google Earth Engine (GEE) platform, while in situ data for monitoring TSS were collected on designated sampling dates. Seasonal satellite composites were generated for the dry season (May–August) and the rainy season (December–March) for each year. In addition, water quality observation data spanning three years were used to validate the suspended solid estimates.

For DO calculations, daily Level-2 data products were employed, including Chl-a concentration, Rrs at multiple wavelengths, and daytime sea surface temperature derived from MODIS-Aqua and VIIRS sensors. MODIS-Aqua Level-1A data for the Krueng Pase Watershed, covering the period 2020–2022, were accessed via the GEE platform.

3 Methods

This study aims to estimate TSS and DO concentrations in the Krueng Pase River Basin using Sentinel-2A satellite imagery from 2020 to 2022, complemented by field observations of sediment yield. Analyses were conducted for both the dry season (May–August) and the rainy season (December–March) to evaluate seasonal variations in TSS distribution.

(a) Atmospheric correction

Sentinel-2A imagery has already undergone geometric adjustments, allowing atmospheric correction to be applied directly. The radiance signal detected by the satellite can be decomposed into several components [21]. The total

reflectance at a specific wavelength λ [22], which is measured at the top of the atmosphere, it can be stated as follows [21–23].

During the correction process, various atmospheric parameters were considered. This adjustment minimizes image distortions by accounting for seasonal factors and local climatic conditions at the time of acquisition, including tropical and subtropical environments. From the Top of Atmosphere (TOA) reflectance values, the correction produces surface reflectance, also referred to as Bottom of Atmosphere (BOA) values.

(b) Masking water body area using Normalized Difference Water Index (NDWI)

The Sentinel-2 Level-1C dataset, which is publicly accessible, provides standard TOA reflectance values that serve as the input imagery data. Therefore, no additional preprocessing is required. When computing the NDWI, TOA reflectance is more appropriate than raw Digital Numbers [24].

Area masking was performed using the NDWI algorithm prior to calculating TSS. This algorithm effectively distinguished water bodies from land and soil, thereby ensuring that only the relevant water areas were included in the analysis. Although NDWI is generally reliable for extracting water information, it is susceptible to interference from built-up areas and may overestimate the size of water bodies. NDWI is calculated as the normalized difference between the Green and Near Infrared (NIR) wavelengths [25, 26], within the following formula:

$$\mathrm{NDWI} = \frac{(\mathrm{Green} - \mathrm{NIR})}{(\mathrm{Green} + \mathrm{NIR})} \tag{1}$$

where,

NIR = Reflectance value for the near infrared channel,

Green = Reflectance value for the surface of the green channel.

(c) Total Suspended Solid (TSS) Algorithm

Rrs data can be applied to develop observational, analytical, and semi-analytical models of suspended sediments using Landsat-8 imagery. For the Krueng Pase Watershed, Laili's algorithm , originally developed for Poteran Island [27], was considered more suitable. This algorithm is an empirical model that utilizes reflectance values. In this study, the algorithm was adapted to Sentinel-2A imagery, which provides a pixel size of 10 m. The relevant channels correspond to wavelengths of 496.6 nm (Rrs2, blue band) and 664.5 nm (Rrs4, red band). The formula below uses the most significant reflectance numbers from the atmospherically corrected between blue and red channels.

$$\mathrm{TSS}\left(\frac{\mathrm{mg}}{\mathrm{L}}\right) = 31.42 \times \frac{\log(\mathrm{Rrs}(496.6))}{\log(\mathrm{Rrs}(664.5))} - 12.719 \tag{2}$$

Consequently, no additional preprocessing is required for these methods, which can be directly applied to extract water information from satellite imagery. The proposed technique for estimating TSS concentrations has consistently produced satisfactory accuracy [28], as demonstrated by relative error values of less than 30%.

(d) Modified Universal Soil Loss Equation (MUSLE)

Erosion is calculated using the Modified Universal Soil Loss Equation (MUSLE) formula with the following variables: rainfall factor, peak discharge (Qp), soil erosion (K), Slope Index (S), Slope Length (L), vegetation cover, and plant cultivation methods in the field (P).

$$\mathrm{A_{MUSLE}} = 11.8(\mathrm{VQ} \times \mathrm{Qp})^{0.56} \times \mathrm{K} \times \mathrm{LS} \times \mathrm{CP} \tag{3}$$

where,

VQ = Flow volume during a rainfall event (m^3),

Qp = Maximum debit (m^3/s),

K = Land Erodibility Factor,

LS = Slope, and

CP = Land use and land management factors.

(e) Dissolved Oxygen (DO)

In this study, the used of empirical algorithm to estimate the Chl-a from MODIS Rayleigh-corrected reflectance (Rrc) value 645 and 859 [29] for normalized spectral index in the study area before using the empirical model of Chl-a as follows.

$$\text{Chl-a} = -1454.3 \times \propto +69.35 \tag{4}$$

The value of $\propto$ was from exponential of Rrc value.

$$\propto = \frac{\left(\mathrm{Exp}\left(\mathrm{R_{rc(645)}}\right) - \mathrm{Exp}\left(\mathrm{R_{rc(859)}}\right)\right)}{\left(\mathrm{Exp}\left(\mathrm{R_{rc(645)}}\right) + \mathrm{Exp}\left(\mathrm{R_{rc(859)}}\right)\right)} \tag{5}$$

To calculate the concentration of DO, it is necessary to first determine the Sea Surface Temperature (SST) using the empirical model as the temperature quantities [30]. In fact, SST, Chl-a and DO concentration exhibit a strong relationship and provide a good interpretability [31].

$$\mathrm{SST}\,(^{\circ}\mathrm{C}) = \mathrm{C}_1 + \mathrm{C}_2\mathrm{T}_{11} + \mathrm{C}_3\,(\mathrm{T}_{11} - \mathrm{T}_{12})\,\mathrm{T}_{\mathrm{sfc}} + \mathrm{C}_4(\sec(\theta) - 1)\,(\mathrm{T}_{11} - \mathrm{T}_{12}) \tag{6}$$

where,

C_1 and C_4 = the MODIS 11–12 μm coefficient of SST,

T_{11} and T_{12} = Brightness temperatures in 11–12 μm, and

$\mathrm{T}_{\mathrm{sfc}}$ = the reference (Reynolds) of SST.

To examine the spatial and temporal distribution of DO in the Krueng Pase Watershed, both in situ measurements and MODIS satellite data were utilized. DO distribution was predicted by integrating water temperature measurements with estimates of Chl-a concentration. This approach enabled the prediction of DO levels across the watershed. The findings indicate that temperature plays a dominant role in determining the amount of oxygen that can dissolve in water, thereby exerting the greatest influence on the DO concentration.

(f) Statistical analysis and validation

In this study, an algorithm based on the computation of suspended variables was applied to verify accuracy. The TSS values derived from Landsat-8 imagery were compared with in situ measurements to ensure reliability. Table 1 presents the validation results, expressed through Nash–Sutcliffe Efficiency (NSE) and Percent Bias (PBIAS) metrics [32].

$$\mathrm{NSE} = 1 - \frac{\sum_{i=1}^{N}(\mathrm{P}_{oi} - \mathrm{P}_{si})^2}{\sum_{i=1}^{N}(\mathrm{P}_{oi} - \mathrm{P}_{mean})^2} \tag{7}$$

$$\mathrm{PBIAS} = \frac{\sum_{i=1}^{N}(\mathrm{P}_{oi} - \mathrm{P}_{si}) \times 100}{\sum_{i=1}^{N}(\mathrm{P}_{oi})} \tag{8}$$

where,

P_{oi} = the ith observation,

P_{si} = the ith of simulated value, and

P_{mean} = Mean observation data for evaluated.

Table 1. Performance ratings of Nash–Sutcliffe Efficiency (NSE) and Percent Bias (PBIAS) [32]

Performance	NSE	PBIAS
Very Good	$0.75 < \mathrm{NSE} \leq 1.00$	$\mathrm{PBIAS} \leq \pm 25$
Good	$0.65 < \mathrm{NSE} \leq 0.75$	$\pm 25 \leq \mathrm{PBIAS} < \pm 40$
Satisfying	$0.50 < \mathrm{NSE} \leq 0.65$	$\pm 40 \leq \mathrm{PBIAS} < \pm 70$
Not Satisfactory	$\mathrm{NSE} \leq 0.50$	$\mathrm{PBIAS} \geq \pm 70$

4 Results and Discussion

4.1 Seasonal Distribution of Total Suspended Solid (TSS)

Rainfall is a crucial factor in estimating runoff and sedimentation. In the Krueng Pase Watershed, the erosion hazard level increased significantly between 2009 and 2019; mild erosion rose by 7.9%, while moderate erosion increased by 27.4%. The highest erosion rates were observed in agricultural land, built-up areas, and mixed agricultural zones. For instance, inceptisol soil types are particularly prone to erosion [33]. Peak discharge and runoff values, which are strongly influenced by rainfall intensity, largely determine erosion rates. Beyond reducing watershed productivity and overall quality, soil erosion diminishes the river's capacity to transport sediments.

Figure 2 illustrates the sediment yield from erosion in the Krueng Pase Watershed, calculated using the MUSLE. The estimated sediment yields were 4,114 tons in 2019, 20,701 tons in 2020, 15,371 tons in 2021, and 22,872 tons in 2022.

Erosion can cause damage both at the site of occurrence and downstream outlets where sediment is deposited. This process reduces the carrying capacity of rivers and reservoirs, thereby significantly affecting the overall water quality. Sediment discharge is influenced by several parameters, including flow velocity, flow rate, and sediment concentration within the channel [34]. The MUSLE, however, has certain limitations, as it can only quantify sedimentation at the plot or outlet scale. Soil erosion also affects soil fertility through the loss of nutrients, which subsequently accumulate in water bodies [35].

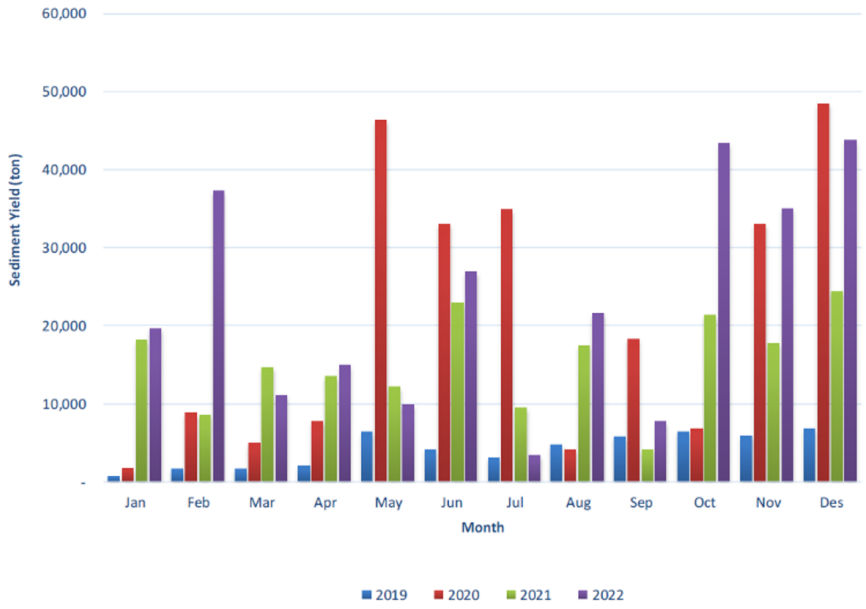

Figure 2. Sediment yield of Krueng Pase Watershed

The spatial distribution of TSS must be thoroughly understood. Sediment is commonly found at the base of mountains, along waterways and rivers, and within reservoirs. Sedimentation refers to the deposition of debris in water as a result of erosion. This process involves the accumulation of earth particles, facilitated by the water flow velocity, which enables the sediment to reach its settling velocity. Prolonged periods of intense rainfall can exacerbate this situation, as sediment accumulation in river bodies reduces their water holding capacity, posing significant hazards.

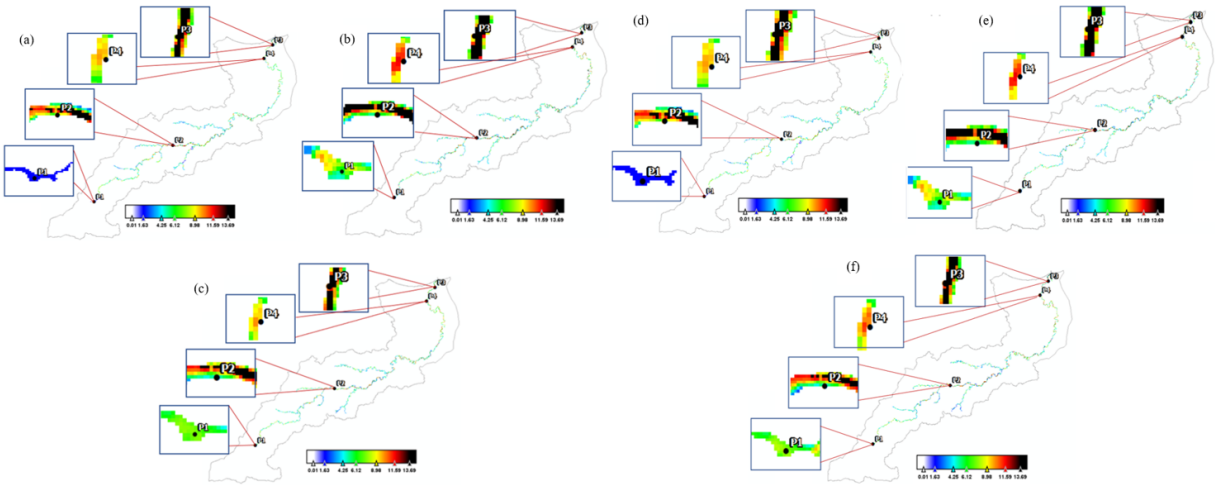

Figure 3. The distribution of Total Suspended Solid (TSS) in Krueng Pase Watershed: (a) Summer 2020; (b) Summer 2021; (c) Summer 2022; (d) Rainy 2020; (e) Rainy 2021 and (f) Rainy 2022

The TSS results obtained from Sentinel-2A data indicate that the downstream region of the watershed consistently experiences elevated levels of suspended solids from 2020 to 2022. Specifically, the TSS concentration exceeded 11 mg/L, which contrasts with the upstream area of the river basin. The upstream region exhibits a lower concentration of suspended solids, as it represents the source of the river flow, resulting in minimal particle transport with a suspended solid value of 1.63 mg/L, as depicted in Figure 3, where values are less than 2 mg/L on the distribution map. This is in contrast to the sections along the river flow, which accumulated erosion levels with values ranging from 4 to 10 mg/L. Figure 3 illustrates the transport of suspended particles from upstream to downstream, with the majority of suspended particles accumulating along the coastal area. The coastal region, which serves as the estuary of the Krueng Pase Watershed, is surrounded by urbanized areas that may contribute to increased river water waste.

Based on the results of the distribution modeling shown in Figure 3, annual observations from 2020 to 2022 using Sentinel-2A satellite imagery with a spatial resolution of 60 m revealed distinct patterns in sedimentation dynamics within the Krueng Pase Watershed. The rise and fall in sedimentation levels were evident, with observational statistics

indicating that sediment concentrations increased each year during the wet season. This trend explains the significant increase in the sediment levels observed at the P4 monitoring site. The locations of the in-situ data collection from the four observation points are presented in Table 2.

Table 2. Location of in-situ data for Total Suspended Solid (TSS) measurement

Point	X	Y
P1	96°54′4″E	4°51′29″N
P2	97°3′40.26″E	4°58′37.38″N
P3	97°13′24.57″E	5°8′22.83″N
P4	97°12′34.69″E	5°7′3.10″N

According to satellite imagery statistics on sediment, there was increasing of sediment value during the rainy season each year by using the TSS algorithm 9.4 mg/L in 2020, 10.6 mg/L in 2021, and 10.7 mg/L more in 2022 (Table 3).

Table 3. In-situ data and observation satellite for Total Suspended Solid (TSS) measurement

Point Insitu Data	2020		2021		2022	
	T1 (mg/L)	T2 (mg/L)	T1 (mg/L)	T2 (mg/L)	T1 (mg/L)	T2 (mg/L)
P1	7.66	8.23	6.40	7.30	8.23	9.06
P2	6.75	7.01	5.03	6.43	7.20	6.80
P3	8.00	5.40	6.85	7.48	5.18	7.75
P4	7.50	8.70	11.00	12.01	6.00	13.21
Point Observation Satellite	**2020**		**2021**		**2022**	
	T1 (mg/L)	**T2 (mg/L)**	**T1 (mg/L)**	**T2 (mg/L)**	**T1 (mg/L)**	**T2 (mg/L)**
P1	1.65	2.50	2.11	2.00	1.90	1.80
P2	6.20	6.30	5.00	6.50	3.31	3.40
P3	6.12	6.20	8.50	8.29	8.10	10.00
P4	9.20	9.40	10.00	10.60	10.20	10.70

In situ data regarding suspended solids were collected at four sampling points within the Krueng Pase watershed, with P1 located upstream and P4 downstream. The first observation period, encompassing both in situ and satellite imagery, occurred from April to May, while the second period extended from August to October.

The average TSS concentration, as determined from observational data or field measurements in the Krueng Pase watershed, was 7.48 mg/L in 2020, 7.32 mg/L in 2021, and 7.65 mg/L in 2022 during period I (T1). For period II (T2), the TSS concentration was 7.33 mg/L in 2020, 8.305 mg/L in 2021, and 8.955 mg/L in 2022. Water turbidity increased during the rainy season.

The TSS values derived from satellite imagery using an algorithm developed with 2020 data were recorded as 6.652 mg/L in 2021, 6.402 mg/L in 2021, and 5.877 mg/L in 2022 for Period I (T1). For Period II (T2), the TSS values were 6.1 mg/L in 2020, 6.847 mg/L in 2021, and 6.475 mg/L in 2022. The validation of observational data against satellite imagery data (Table 4) yielded a NSE of 0.949 (very good) for Period I and 0.645 (satisfactory) for Period II. Additionally, the PBIAS test results indicated values of 15.668 (very good) for Period I and 21.0307 (very good) for Period II.

Table 4. Value interpretation of Nash–Sutcliffe Efficiency (NSE) and Percent Bias (PBIAS)

Time	NSE	Performance	PBIAS	Performance
Period I (T1)	0.949	Very Good	15.6685	Very Good
Period II (T2)	0.645	Satisfying	21.0307	Very Good

As a result, one significant element was TSS. Physicochemical and biological alterations are a result of deteriorating water quality. Physical modifications include adding solids (both organic and inorganic materials) to water, which raises turbidity and further reduces solar entry into water bodies. The NSE is a normalized statistic that determines the relative magnitude of the residual variance (“noise”) compared to the measured data variance (“information”). The PBIAS measures the average tendency of the simulated data to be larger or smaller than their observed counterparts. The NSE value during Period II was classified as satisfactory, indicating good model performance, as values exceeding 0.65 are generally considered acceptable. Prolonged and intense rainfall can significantly increase the pollution load

due to surface runoff and soil erosion, which transports sediment particles into receiving water bodies. This process often results in relatively higher turbidity levels than those observed during the dry season.

4.2 Dissolved Oxygen (DO) as Water Quality Indicator

Regarding the DO results, the average DO trend decreased over three years. As illustrated in the chart, the DO value in 2020 was 7.56 mg/L, which is nearly 7.6 mg/L. It decreased slightly to 7.45 mg/L in early 2021 and then increased to 7.5 mg/L in the middle of that year. In early 2022, the final year of satellite observation data, the DO value was 7.23 mg/L, which continued to decline. The DO levels fluctuated between 5 and 15 mg/L annually, with dry season exhibiting the lowest average concentrations and rainy season the highest, indicating significant seasonal variability. In the summer season, the value of DO was 7.2 mg/L in 2020 and 2021, and in 2022, it was below 7.1 mg/L. This was quite different in the rainy season, with a high DO value. DO is closely related to water temperature. The temperature of the water affects its oxygen content.

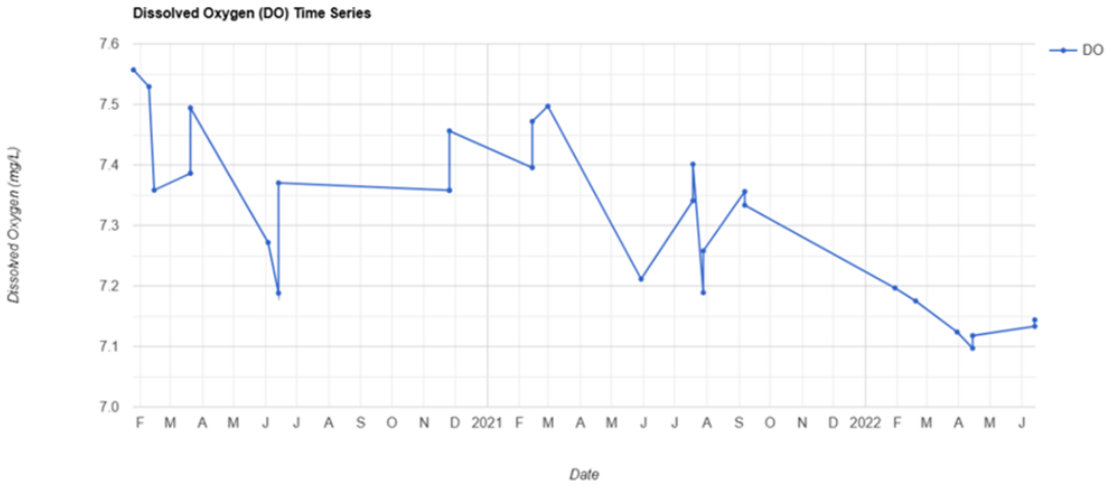

Figure 4. Dissolved Oxygen (DO) chart of 2020 to 2022 remote sensing observation

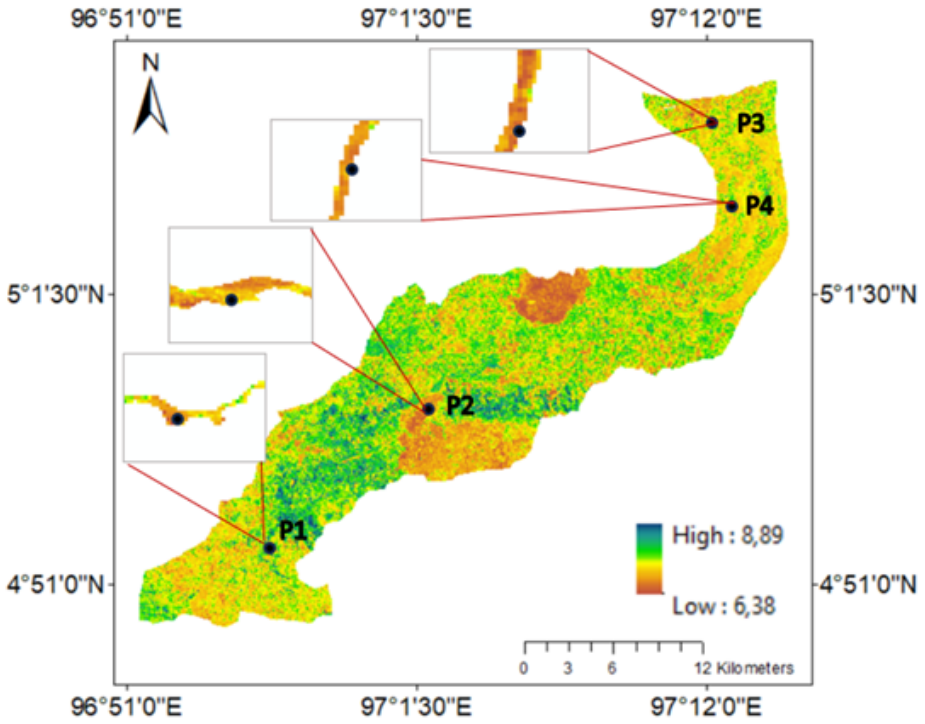

Figure 5. Average Dissolved Oxygen (DO) distribution in Krueng Pase Watershed in 2020 to 2022

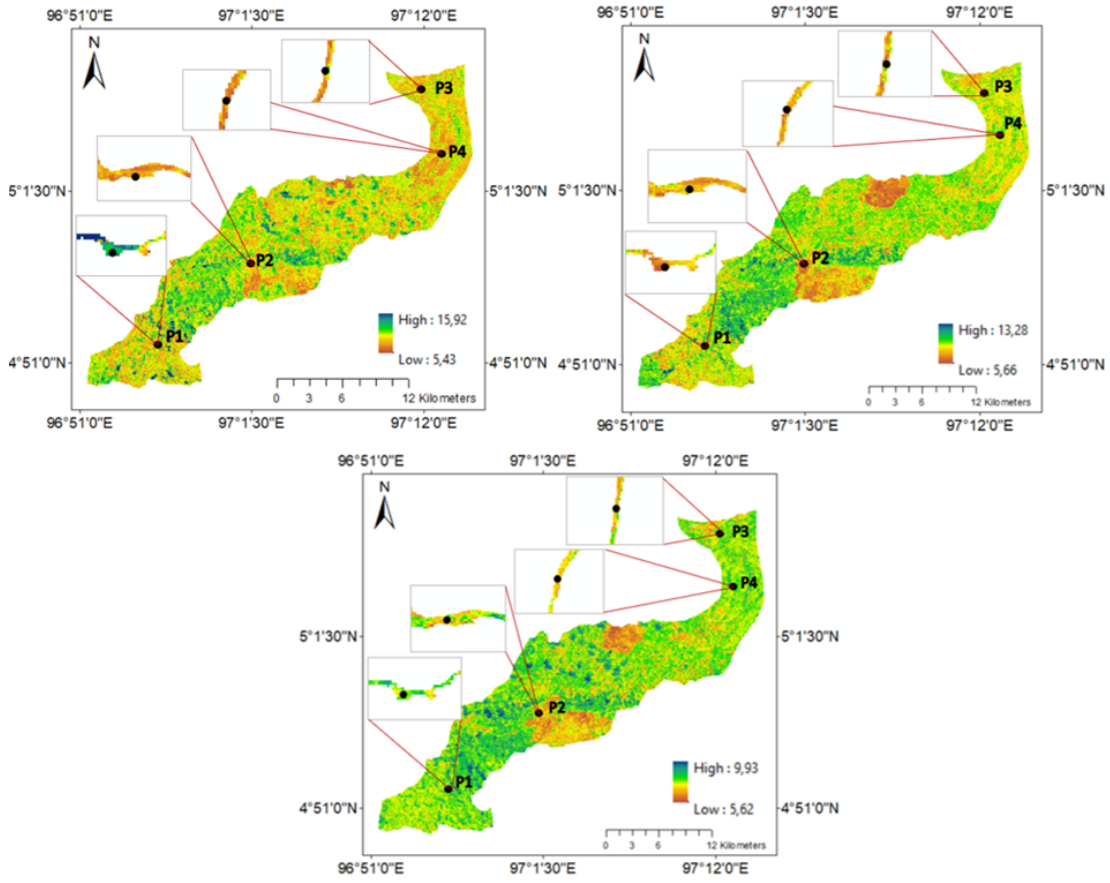

Figure 6. Dissolved Oxygen (DO) distribution map: (a) DO in 2020; (b) DO in 2021; and (c) DO in 2022

Decreasing DO levels in a body of water indicate the decomposition of organic matter and the production of gas. However, in Krueng Pase, the DO value did not experience a drastic decrease (Figure 4). However, this reduction occurred over 3 years, as there was a fluctuation in value without a significant decrease. The average DO distribution from 2020 to 2021 had a high value of 8.89 mg/L (Figure 5) and mapping of DO distribution (Figure 6). Population density has led to the opening of new land, which previously had dense vegetation that provided anti-runoff barriers during the rainy season.

This has led to climate volatility, which could lead to rising surface temperatures and higher rainfall and runoff intensities, potentially leading to hydrological disasters. Consequently, ecosystem disruption will increase significantly due to urbanization and climate change. The air quality index can be clearly observed in the increasing trends of runoff height and rainfall. Water pollution occurs due to the emergence of biota that contaminate water. Furthermore, soil erosion has resulted in large amounts of river water in already polluted watersheds.

Therefore, based on the DO values, the water levels in the Krueng Pase watershed area were not polluted. The pollution levels were minimal because the oxygen value was still sufficient, as the solubility of oxygen and the amount of oxygen in the water increased. As with TSS and DO, both indicators are greatly influenced by agricultural runoff, so that most of the time during the rainy season, the condition of the vegetated forest area and the agricultural rice field area in the middle of the Krueng Pase Watershed is disturbed in its ecosystem.

The decreasing trend in oxygen levels within the Krueng Pase Watershed is evident annually. A consistent decline was observed each year. The highest oxygen level recorded in 2020 was 15.92 mg/L, followed by a decrease to 13.28 mg/L in 2021 and a further significant drop in 2022. This decline negatively impacts the oxygen levels in the water, hindering the productive survival of marine biota that require a DO value above 5 mg/L. Despite this, in 2022, the Krueng Pase Watershed still had an area with a DO value of 9.93 mg/L, which was the highest pixel value, indicating the presence of remaining freshwater zones. Although the lowest DO values in the Krueng Pase Watershed have not yet fallen below 5 mg/L, several pixels approached this critical threshold.

5 Conclusions

Erosion occurs after a period of heavy rainfall. Sediment is produced by erosion and settles at the bottom of waterways, canals, and reservoirs. TSS is composed of silt, fine sand, domestic/industrial waste, and microorganisms, and is carried into water bodies by soil erosion. Suspended and dissolved materials in natural water are typically

nontoxic. However, if present in large quantities, they can increase turbidity, which eventually prevents sunlight from penetrating the water column and affects photosynthesis. Based on these findings, it can be concluded that the sediment yield can be calculated annually using the MUSLE formula as an empirical formula. The calculated value of sediment at the four locations using satellite observations and field measurements was then supported by the estimated value of suspended solids. The amount of suspended sediment along the watershed had a range of values less than 14 mg/L, showing results categorized as very good and satisfying in the NSE accuracy test results. In the accuracy test, the PBIAS results showed that both the dry and rainy seasons were categorized as very good. To strengthen the estimation of water quality using other parameters, the calculation of DO values alone is sufficient to indicate the water conditions in the Krueng Pase. This occurs when DO is estimated using water temperature and chl-a parameters, and DO results exceeding 5 mg/L indicate water capable of supporting a healthy aquatic environment for aquatic biota. Satellite imagery-based algorithms for sedimentation and DO values provide valuable data for land and water management planning. Mapping the distribution of sedimentation and DO as key water quality indicators facilitates evidence based decision making and policy development, helping to ensure the long-term sustainability of the watershed ecosystem.

Author Contributions

Conceptualization and design of the research, I.R. and A.I.; Methodology, I.R. and B.B.; Software and formal analysis A.I.; writing—original draft preparation, I.R.; writing—review and editing, A.I.; visualization, B.B. All authors have read and agreed to the published version of the manuscript.

Funding

This paper was supported by Universitas Syiah Kuala join collaboration with Universitas Hasanuddin (Grant No.: 167/UN11/SPK/PNBP/2021).

Data Availability

The data used to support the findings of this study are available from the corresponding author upon request.

Acknowledgment

The authors extend their deepest appreciation for this work supported by Universitas Syiah Kuala join collaboration with Universitas Hasanuddin for their unwavering support and the generous research grant, 19 February 2021, which made this research feasible.

Conflicts of Interest

The authors declare that they have no conflicts of interest.

References

[1] É. H. Cremon, A. M. S. da Silva, and O. C. Montanher, "Estimating the suspended sediment concentration from TM/Landsat-5 images for the Araguaia River–Brazil," *Remote Sens. Lett.*, vol. 11, no. 1, pp. 47–56, 2020. https://doi.org/10.1080/2150704X.2019.1681597

[2] I. Ramli, A. Achmad, H. Basri, and A. Izzaty, "Erosion and distribution of total suspended sediment (TSS) using Landsat-8 in Krueng Pase watershed," in *Lecture Notes in Civil Engineering*. Singapore: Springer Nature Singapore, 2022. https://doi.org/10.1007/978-981-16-7949-0_3

[3] H. B. Waseem and I. A. Rana, "Floods in Pakistan: A state-of-the-art review," *Nat. Hazards Res.*, vol. 3, no. 3, pp. 359–373, 2023. https://doi.org/10.1016/j.nhres.2023.06.005

[4] D. Y. Xu, B. Gao, X. H. Wan, W. Q. Peng, and B. H. Zhang, "Influence of catastrophic flood on microplastics organization in surface water of the Three Gorges Reservoir, China," *Water Res.*, vol. 211, p. 118018, 2022. https://doi.org/10.1016/j.watres.2021.118018

[5] M. Y. Zhu, J. W. Wang, X. Yang, Y. Zhang, L. Y. Zhang, H. Q. Ren, B. Wu, and L. Ye, "A review of the application of machine learning in water quality evaluation," *Eco-Environ. Health*, vol. 1, no. 2, pp. 107–116, 2022. https://doi.org/10.1016/j.eehl.2022.06.001

[6] G. S. Bilotta and R. E. Brazier, "Understanding the influence of suspended solids on water quality and aquatic biota," *Water Res.*, vol. 42, no. 12, pp. 2849–2861, 2008. https://doi.org/10.1016/j.watres.2008.03.018

[7] A. G. Dekker, R. J. Vos, and S. W. M. Peters, "Comparison of remote sensing data, model results and in situ data for total suspended matter (TSM) in the southern Frisian lakes," *Sci. Total Environ.*, vol. 268, no. 1–3, pp. 197–214, 2001. https://doi.org/10.1016/S0048-9697(00)00679-3

[8] A. Izzaty and B. M. Sukojo, "Identification of land criticality with the application of deep learning in West Lahat district using Sentinel-2A imagery," *IOP Conf. Ser.: Earth Environ. Sci.*, vol. 936, no. 1, p. 012009, 2021. https://doi.org/10.1088/1755-1315/936/1/012009

[9] K. Rangzan, M. Kabolizadeh, and D. Karimi, "Improved water quality mapping based on cross-fusion of Sentinel-2 and Landsat-8 imageries," *IET Image Process.*, vol. 14, no. 7, pp. 1382–1392, 2020. https://doi.org/10.1049/iet-ipr.2019.1503

[10] O. Bozorg-Haddad, M. Delpasand, and H. A. Loáiciga, "Water quality, hygiene, and health," in *Economical, Political, and Social Issues in Water Resources*. Elsevier, 2021, pp. 217–257. https://doi.org/10.1016/b978-0-323-90567-1.00008-5

[11] H. B. Yang, J. L. Kong, H. H. Hu, Y. Du, M. Y. Gao, and F. Chen, "A review of remote sensing for water quality retrieval: Progress and challenges," *Remote Sens.*, vol. 14, no. 8, p. 1770, 2022. https://doi.org/10.3390/rs14081770

[12] M. Shen, H. T. Duan, Z. G. Cao, K. Xue, T. C. Qi, J. G. Ma, D. Liu, K. S. Song, C. L. Huang, and X. Y. Song, "Sentinel-3 OLCI observations of water clarity in large lakes in eastern China: Implications for SDG 6.3.2 evaluation," *Remote Sens. Environ.*, vol. 247, p. 111950, 2020. https://doi.org/10.1016/j.rse.2020.111950

[13] A. Riadi, R. Triatmadja, and N. Yuwono, "Study of total suspended solids (TSS) distribution and salinity of coastal area using satellite imagery for pond development in pond irrigation areas (DIT) Sei Teras," in *International Conference on Sustainable Environment, Agriculture and Tourism (ICOSEAT 2022)*, Bangka, Indonesia, 2022, pp. 172–178. https://doi.org/10.2991/978-94-6463-086-2_23

[14] S. Novoa, D. Doxaran, A. Ody, Q. Vanhellemont, V. Lafon, B. Lubac, and P. Gernez, "Atmospheric corrections and multi-conditional algorithm for multi-sensor remote sensing of suspended particulate matter in low-to-high turbidity levels coastal waters," *Remote Sens.*, vol. 9, no. 1, p. 61, 2017. https://doi.org/10.3390/rs9010061

[15] D. Doxaran, J. M. Froidefond, and P. Castaing, "A reflectance band ratio used to estimate suspended matter concentrations in sediment-dominated coastal waters," *Int. J. Remote Sens.*, vol. 23, no. 23, pp. 5079–5085, 2002. https://doi.org/10.1080/0143116021000009912

[16] S. V. Balasubramanian, N. Pahlevan, B. Smith, C. Binding, J. Schalles, H. Loisel, D. Gurlin, S. Greb, K. Alikas, M. Randla, and et al., "Robust algorithm for estimating total suspended solids (TSS) in inland and nearshore coastal waters," *Remote Sens. Environ.*, vol. 246, p. 111768, 2020. https://doi.org/10.1016/j.rse.2020.111768

[17] L. F. Arias-Rodriguez, Z. Duan, J. D. J. Díaz-Torres, M. Basilio Hazas, J. Huang, B. U. Kumar, Y. Tuo, and M. Disse, "Integration of remote sensing and Mexican water quality monitoring system using an extreme learning machine," *Sensors*, vol. 21, no. 12, p. 4118, 2021. https://doi.org/10.3390/s21124118

[18] Y. H. Kim, S. Son, H. C. Kim, B. Kim, Y. G. Park, J. Nam, and J. Ryu, "Application of satellite remote sensing in monitoring dissolved oxygen variabilities: A case study for coastal waters in Korea," *Environ. Int.*, vol. 134, p. 105301, 2020. https://doi.org/10.1016/j.envint.2019.105301

[19] H. Guo, J. J. Huang, X. Zhu, B. Wang, S. Tian, W. Xu, and Y. Mai, "A generalized machine learning approach for dissolved oxygen estimation at multiple spatiotemporal scales using remote sensing," *Environ. Pollut.*, vol. 288, p. 117734, 2021. https://doi.org/10.1016/j.envpol.2021.117734

[20] H. Wibisana, B. Aryaseta, and P. C. Wardhani, "Analysis of dissolved oxygen on Tuban coast using remote sensing algorithms from Landsat 8 satellite image data and interpolated polynomials," *Rev. Gestão Soc. Ambient.*, vol. 18, no. 8, pp. 1–13, 2024. https://doi.org/10.24857/rgsa.v18n8-049

[21] Q. T. Bui, C. Jamet, V. Vantrepotte, X. Mériaux, A. Cauvin, and M. A. Mograne, "Evaluation of Sentinel-2/MSI atmospheric correction algorithms over two contrasted French coastal waters," *Remote Sens.*, vol. 14, no. 5, p. 1099, 2022. https://doi.org/10.3390/rs14051099

[22] H. R. Gordon, "Atmospheric correction of ocean color imagery in the Earth Observing System era," *J. Geophys. Res. Atmos.*, vol. 102, no. D14, pp. 17 081–17 106, 1997. https://doi.org/10.1029/96jd02443

[23] H. R. Gordon and M. Wang, "Retrieval of water-leaving radiance and aerosol optical thickness over the oceans with SeaWiFS: A preliminary algorithm," *Appl. Opt.*, vol. 33, no. 3, p. 443, 1994. https://doi.org/10.1364/ao.33.000443

[24] B. Ko, H. Kim, and J. Nam, "Classification of potential water bodies using Landsat 8 OLI and a combination of two boosted random forest classifiers," *Sensors*, vol. 15, no. 6, pp. 13 763–13 777, 2015. https://doi.org/10.3390/s150613763

[25] S. K. McFeeters, "The use of the Normalized Difference Water Index (NDWI) in the delineation of open water features," *Int. J. Remote Sens.*, vol. 17, no. 7, pp. 1425–1432, 1996. https://doi.org/10.1080/01431169608948714

[26] X. Yang, S. Zhao, X. Qin, N. Zhao, and L. Liang, "Mapping of urban surface water bodies from Sentinel-2 MSI imagery at 10 m resolution via NDWI-based image sharpening," *Remote Sens.*, vol. 9, no. 6, p. 596, 2017. https://doi.org/10.3390/rs9060596

[27] N. Laili, F. Arafah, L. M. Jaelani, L. Subehi, A. Pamungkas, E. S. Koenhardono, and A. Sulisetyono, "Development of water quality parameter retrieval algorithms for estimating total suspended solids and

chlorophyll-A concentration using Landsat-8 imagery at Poteran island water," *ISPRS Ann. Photogramm. Remote Sens. Spatial Inf. Sci.*, vol. II-2/W2, pp. 55–62, 2015. https://doi.org/10.5194/isprsannals-II-2-W2-55-2015

[28] L. M. Jaelani, B. Matsushita, W. Yang, and T. Fukushima, "Evaluation of four MERIS atmospheric correction algorithms in Lake Kasumigaura, Japan," *Int. J. Remote Sens.*, vol. 34, no. 24, pp. 8967–8985, 2013. https://doi.org/10.1080/01431161.2013.860660

[29] K. Shi, Y. L. Zhang, G. W. Zhu, B. Q. Qin, and D. L. Pan, "Deteriorating water clarity in shallow waters: Evidence from long term MODIS and in-situ observations," *Int. J. Appl. Earth Obs. Geoinf.*, vol. 68, pp. 287–297, 2018. https://doi.org/10.1016/j.jag.2017.12.015

[30] M. Liu, L. Wang, and F. D. Qiu, "Using MODIS data to track the long-term variations of dissolved oxygen in Lake Taihu," *Front. Environ. Sci.*, vol. 10, p. 1096843, 2022. https://doi.org/10.3389/fenvs.2022.1096843

[31] L. Dong, D. Wang, L. Song, F. Gong, S. Chen, J. Huang, and X. He, "Monitoring dissolved oxygen concentrations in the coastal waters of Zhejiang using Landsat-8/9 imagery," *Remote Sens.*, vol. 16, no. 11, p. 1951, 2024. https://doi.org/10.3390/rs16111951

[32] D. N. Moriasi, J. G. Arnold, M. W. Van Liew, R. L. Bingner, R. D. Harmel, and T. L. Veith, "Model evaluation guidelines for systematic quantification of accuracy in watershed simulations," *Trans. ASABE*, vol. 50, no. 3, pp. 885–900, 2007. https://doi.org/10.13031/2013.23153

[33] Muntazar, Joni, and I. Ramli, "Erosion and sedimentation analysis due to land use changes in the Krueng Pase watershed," *IOP Conf. Ser. Earth Environ. Sci.*, vol. 922, no. 1, p. 012040, 2021. https://doi.org/10.1088/1755-1315/922/1/012040

[34] G. H. Syamsuddin, M. S. Pallu, F. Maricar, and B. Bakri, "Analysis of the seasonal change on the sediment transport in the primary channel of Saddang irrigation area," *Eng. Technol. Appl. Sci. Res.*, vol. 15, no. 1, pp. 20 138–20 143, 2025. https://doi.org/10.48084/etasr.9575

[35] L. Zhang, M. Haseeb, Z. Tahir, A. Tariq, K. F. Almutairi, and W. Soufan, "Assessment of soil erosion dynamics and implications for sustainable land management: A case study using the RUSLE model," *Int. J. Sediment Res.*, vol. 40, no. 3, pp. 385–399, 2025. https://doi.org/10.1016/j.ijsrc.2024.12.001